Intrinsic Paramagnetic Defects Probe the Superionic Phase Transition in Mechanochemically Synthesized AgI Nanocrystals

D. Bharathi Mohan and C. S. Sunandana*

School of Physics, University of Hyderabad, Hyderabad 500 046, Andhra Pradesh, India

Received: September 27, 2005; In Final Form: January 18, 2006

Electron paramagnetic resonance (EPR) of two intrinsic paramagnetic centers generated by soft mechanochemistry of Ag and I to yield zinc blende γ-AgI nanoparticles ($\sim$38 nm) has been used for the first time to probe the $\gamma-\alpha$ (body centered cubic) superionic phase transitions in AgI at (423 $\pm$ 1) K. These results are agreeable with the differential scanning calorimetric studies. A transmission electron microscope picture shows the average crystallite size in the range of $\sim$30−40 nm. A hole-type Ag-related paramagnetic center (Ag^{2+}) with an average $g = 2.21025$ value is remarkably sensitive to the first-order phase transition exhibiting sharp drops at the phase transition temperature (T_t) and complete reversibility. The T_t is characterized by a sharp, abrupt rise in the inverse paramagnetic susceptibility $1/\chi$ by 1 order (7.4×10^{10} to 3.17×10^{11} in kg m^{-3}) which reflects changes in the bonding of the material. Furthermore, a sharp signal at $\langle g \rangle = 2.0019$ ($\Delta H_{PP} =$ 10 G) due to an electron-excess center (Ag^0) as a result of Ag metal nanoclusters also formed during the mechanochemical reaction (MCR) yields an abrupt and drastic decrease in the intensity observed at $T_t = 423$ K. From high-temperature (323 to 433 K) $I-V$ characteristics, the evolution of nonohmic behavior is observed on the order of $10^{-9}-10^{-6}$ A with increasing temperature until below T_t which becomes ohmic thereafter. The reason could be the creation of an electronic defect such as Ag^0 metal nanoclusters formed during the near-equilibrium mechanochemical reaction, with the increased excess free energy favoring the formation of γ-AgI nanoparticles.

Introduction

Superionic materials are ionic solids whose conductivities at ambient temperatures are of the order of molten salt electrolytes.[1] To realize superionic conductivity, it is necessary to increase the number of defects such as Frenkel defects, that is, vacancies and interstitials, and to lower the activation energy for ion jump in an ionic material. AgI, an Ag^+ ion conductor, is an example where both these criteria are naturally fulfilled. It exhibits the well-known first-order-type phase transition at 419 K from a stable hexagonal structure or a metastable zinc blende structure with moderate conductivity to the high conductivity state with cubic structure and a higher density compared to low temperature. In the superionic ($\sigma \sim 10^{-2}$ S/cm) state, AgI adopts an I-based body centered cubic (bcc) structural framework in which a heavily disordered ("molten") Ag^+ sublattice is accommodated. The exact origin of this phase transition, as also the nature of the ionic motion in the superionic phase, is still an open question. Aniya and Ichihara performed a critical study of superionic phase transition temperature models based on defect−defect interactions and concluded that to correctly model the phenomena one must also consider electron subsystem and ion−electron interactions.[2] A cluster-induced distortion model in a modified lattice gas approach reproduces the $\sigma(T)$ curve as well, and this model rightly emphasizes the electronic subsystem—although in a subtle manner.[3] In view of this, it would be of interest to look for electron/hole-based defects in AgI that could probe the superionic phase transition.

In a recent work, we have synthesized AgI−CuI solid solutions by a physicochemical process such as a soft mechanochemical reaction (MCR) involving Ag, Cu, and I and studied their structure, thermal stability, and electronic conductivity.[4] During the MCR, both ionic, that is, Ag^+ vacancies and interstitials and electronic defects such as Ag^{2+} and Ag^0 (metallic clusters) are probably formed at the surfaces/interfaces. Relaxation of these defects produced and stabilized in very large numbers under near-equilibrium thermodynamic conditions could yield paramagnetic complexes. EPR is a local microscopic resonance spectroscopic probe that can detect Ag^{2+} and Ag^0 which are paramagnetic species formed during a soft MCR involving Ag and I. It is well established that mechanical activation of solids leads to the formation of structural and electronic defects some of which could exhibit paramagnetic behavior.[5,6] Though many workers[7−17] have detected atomic Ag^0 centers and hole Ag^{2+} centers in different systems, to our knowledge, there is no report on the EPR of Ag^{2+} centers or complexes (or for that matter any other paramagnetic impurity) in AgI created by any means.[18] If such centers were to be created, then they could serve as an excellent direct microscopic probe of the superionic phase transition especially because the more extended (compared to $3d^9$ of Cu^{2+}) $4d^9$ configuration of Ag^{2+} could very effectively and sensitively probe structural and ion dynamical changes associated with the phase transition.

In this work, we report two intrinsic paramagnetic centers: an Ag^{2+}-based hole center and an Ag-based conduction electron center associated with AgI nanocrystallites by using EPR as a probe. Most interestingly, the EPR probe has turned out to be a remarkable sensor of the first-order phase transition of AgI from the zinc blende phase to the high-temperature cubic phase. EPR is potentially capable of characterizing surface species formed in heterogeneous electron transfer reactions at metal surfaces and semiconductor surfaces/interfaces that naturally

* To whom correspondence should be addressed. E-mail: csssp75@yahoo.co.in. Tel: +91-40-23010883 (res.); +91-40-23134324 (off.) Fax: +91-40-23010227.

10.1021/jp055497j CCC: $33.50
Published on Web 02/11/2006

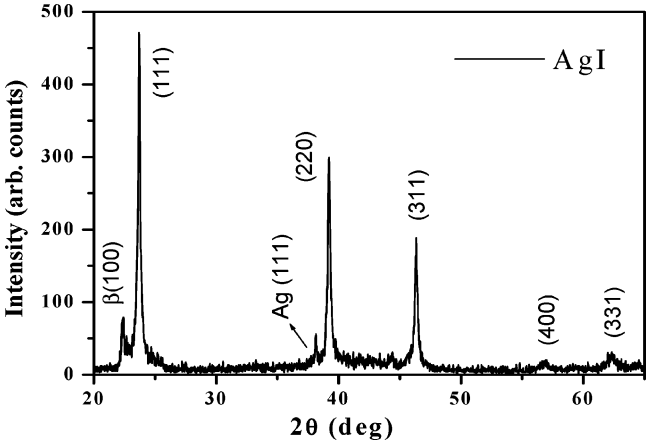

Figure 1. XRD pattern of AgI nanocrystallites obtained by MCR.

occur in nanocomposites. For the first time, the structural phase transition of AgI from the normal to fast ion conducting phase is studied for mechanically ground undoped AgI nanocrystallites using EPR as a probe. The "MCR" is a simple, interesting, soft physicochemical process for synthesizing nanomaterials for applications such as catalysis, electrochemical sensors, electronic device fabrication, and micropower batteries without further processing.

Experimental Methods

AgI was synthesized by mechanical grinding of Ag and I in a 6 in. agate mortar and pestle for 7 h at room temperature in an unilluminated room. Appropriate quantities (in wt %) of polycrystalline silver (Special Materials Project, Hyderabad, India, 99.9% pure) and iodine flakes (Rasayana Laboratory, India, 99.9% pure) were used. Structural characterization on this as-synthesized sample was performed using a PHILIPS diffractometer with Cu Kα1 radiation. For transmission electron microscope (TEM) measurements, first, the samples were made as a colloidal suspension in tetrahydrofuran (THF). Then, 3 mm copper (Cu) grids (400 mesh size) were coated with collodion and then with carbon to enhance the conductivity. An amount of 1−2 drops of sample was placed on this collodion and carbon-coated grids and allowed for drying. These grids were examined with a JEOL-JEM 100CX-II transmission electron microscope at an operating voltage of 80 kV. EPR spectra were obtained from a sample contained 4 mm quartz tube. A JEOL JES-FA 200 X-band EPR spectrometer was used to acquire the spectra. JEOL DVT controller was used (150 to 463 K) for controlling the temperature while heating and cooling. The spectrometer settings used in recording the spectra were as follows: modulation frequency is 100 kHz, modulation amplitude is 10 G, frequency is 9.159665 GHz, and power is 0.99800 mW.

Results and Discussions

Crystal Structure, Particle Size, and Thermal Stability. The X-ray diffraction (XRD) pattern of (Figure 1) "as-prepared" undoped AgI reveals the presence of a mixture of two phases: the major γ-AgI (sphalerite or zinc blende structure, approximately 95%) phase, characterized by the XRD peaks (111), (220), (311), (400), and (331) ($a = 649$ pm), and the minor β-AgI (Wurtzite structure, approximately 5%) phase identified by (100) reflections ($a = 412$ pm, $c = 730$ pm). The average crystallite size of γ-AgI (~38 nm) was determined from the full width at half-maximum (fwhm) of the three predominant peaks (111), (220), and (311) using the Scherrer formula, $t = [(0.9\lambda)/(B \cos \theta)]$.[19] The use of the Lorentzian function to fit the fwhm of three peaks yields more accurate (error is approximately 0.22%) results than those obtained by using Gaussian (1%) and Voigt functions (0.5%). Therefore, the observed XRD lines are essentially Lorentzian, pointing to a uniform crystallite size distribution. Moreover, it detects Ag-(111), signaling the formation of Ag nanoparticles produced by MCR upon prolonged grinding which is a favorable reaction for stabilizing γ-AgI nanoparticles with an intrinsic nonstoichiometry such that [Ag/I] ≥ 1. It also suggests that the iodine atom has little effect on the electronic configuration of the (111) surface atoms. This can be reasoned as the coordination number, that is, 9, which is very close to the bulk-like coordination.[20] Consequently, a very sharp signal with much less intensity observed at 3260 G is obtained in the EPR absorption spectrum as discussed in detail later.

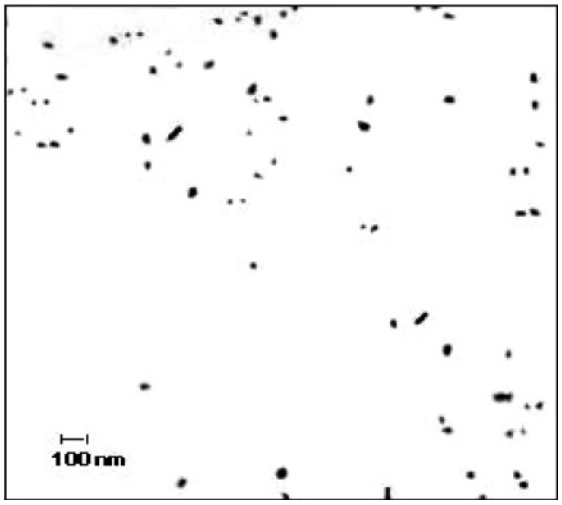

Figure 2. Transmission electron micrograph of 7 h MCR-derived AgI (bigger dark spots) and Ag (smaller gray spots) nanocrystallites.

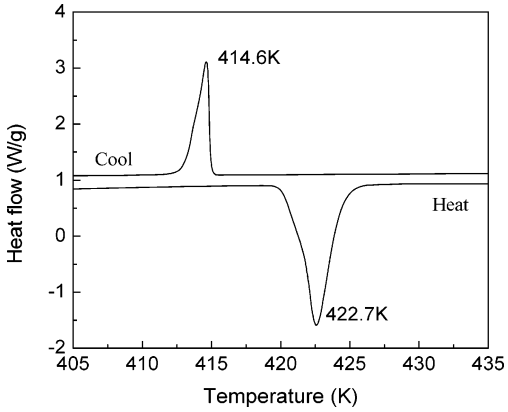

Figure 3. DSC curve shows the phase transition temperature (T_t) at 422.7 K while heating AgI nanoparticles, whereas in cooling, T_t is observed at 414.6 K. The transition enthalpy is 1158 R.K.

Figure 2 shows the transmission electron micrograph of a mechanically reacted ground sample of γ-AgI and unreacted Ag nanocrystallites where bigger and dark spots are γ-AgI and smaller spots are Ag crystallites. The average crystallite size of γ-AgI is about 40 nm which is in accordance with the average crystallite size calculated from XRD. The main purpose of grinding was to stabilize the metastable zinc blende structure of γ-AgI as well as to reduce the particle size. Figure 3 shows the thermal response of an MCR-derived AgI solid solution scanned at a rate of 10 K/min in nonisothermal mode.

When AgI was heated from 400 to 435 K, a very broad and endothermic peak, characterizing the $\gamma \rightarrow \alpha$-AgI (zinc blende to cubic) phase transition temperature (T_t), is observed at 422.7 ($\pm$1) K. This basic thermodynamic result is appreciably comparable with the temperature dependence of the electrical conductivity,[21] lattice parameters,[22] heat capacity,[23] thermal expansion,[24] and magnetic susceptibility[25] of both experimental and theoretical values which put the $\gamma \rightarrow \alpha$-AgI phase transition temperature at 422 K. AgI is cation disordered even at room temperature and also a weakly covalent bonded structure. MCR possibly strengthens the AgI bond in addition to increasing the number of Frenkel defects which leads to the accumulation of local strain at the grain level, besides increased surface area, especially at the nanoscale level. The transition enthalpy is 1158 R.K., calculated by using $\Delta H = kA/m$, where k is the calibration constant, A is the area under the curve, and m is the mass of the sample.[4] This value is very close to the total enthalpy (1150 R.K. where R = gas constant) calculated by Shaviv et al. from specific heat measurements,[26] which reveal the presence of Frenkel defects induced by the MCR process.

Superionic Phase Transition through EPR. When MCR-synthesized AgI nanocrystallites are heated up to 463 K and cooled back to room temperature, the EPR spectrum changes as shown in parts a and b of Figure 4. Two signals, the predominant asymmetric broad signal at a resonance magnetic field of 2960 G (signal A) and a weak, sharp resonance (3260 G) (signal B), are observed at room temperature. Note that commercial AgI does not exhibit any EPR spectrum because it possesses only diamagnetic susceptibility. Takahashi has performed a measurement on susceptibility through phase transition which shows that the AgI goes from the low-temperature more diamagnetic phase to a high-temperature less diamagnetic phase.[25] Signals "A" and "B" arise from the paramagnetic centers nucleated and stabilized during the course of the MCR leading to the formation of γ-AgI. These centers are intrinsic in this case and can undergo a valance state change upon trapping a carrier. The possible paramagnetic centers are Ag^{2+} in (pseudo) tetrahedral surroundings and Ag^0: trapping of a hole by Ag^+ gives rise to Ag^{2+} while trapping of an electron by Ag^+ results in Ag^0. The trapped hole center is in the nature of a complex whose symmetry and concentration decides the EPR spectrum. It is known that Ag(II) complexes are formed by disproportionation of Ag(I) into Ag(II) and Ag(0)[27] and MCRs could support such a process. A large concentration of such "complexes" could lead to (a) unresolved g and hyperfine anisotropies and (b) asymmetric line shapes and large line widths, the former is due to the asymmetry of the complex and the latter is due to dipolar interactions**.** A detailed discussion about the hole center is given in the next section. An abrupt change in signal "A" is observed at 423 ($\pm$1) K that is the characteristic of $\gamma \rightarrow \alpha$-AgI (zinc blende to body centered cubic) superionic phase transition; while upon cooling, the signal is retraced confirming the reversibility which is in accordance with DSC results. Note that our earlier attempts to probe the phase transitions by EPR, in AgI thin film, foils, and nanosized powders prepared by novel methods[28,29] were unsuccessful. Signal "A" corresponding to Ag^{2+} is a $4d^9$ system just as Cu^{2+} is a $3d^9$ system. However, the more extended 4d electron in Ag^{2+} makes it more sensitive to movements of its neighbors. Thus, an ESR study of the Ag^{2+} complex is expected to be sensitive to structural phase transition in general and superionic phase transition in AgI nanocrystallites derived by MCR.

Hole Center (Ag^{2+}). Signal "A" at $\langle g \rangle = 2.21025$ ($g > 2.0036$) and $\Delta H \approx 1000$ G arises essentially from a hole-type paramagnetic center. The averaging of the axially symmetric g tensor (usually observed for the "dilute" Ag^{2+} system) and the rather large line width observed besides the absence of the Ag hyperfine structure in the present case are features that must be attributed to the special nature of the mechanochemical reaction process and the possible effects of nanocrystallite size and/or shape. Positively charged Ag^{2+} ($4d^9$) involving various degrees of hole trapping are possibly generated during the reaction, $Ag + (^1/_2)I_2 \rightarrow AgI$, driven by the shearing of Ag grains and diffusion of iodine across fresh surfaces and interfaces generated during the MCR process. The observed resonance could be the result of a large number of "frozen" paramagnetic clusters stabilized under near-equilibrium conditions that increase excess free energy of the system. Under these conditions, the defect formation and structure stabilization are controllable. Progressive grinding could produce randomly local minima in order to stabilize an Ag^+−ligand charge transfer in these processes. It is this local equilibrium and slight departure from overall equilibrium that favors Ag^{2+} formation. Among silver halides, only AgF_2 has intrinsic Ag^{2+} as part of its lattice, as revealed through powder neutron diffraction studies[30] to be an $S = {}^1/_2$ antiferromagent with a T_N of 163 K and to exhibit a weak 4d ferromagnetism below that temperature. Irradiation does not seem to produce Ag^{2+} in AgI. Unusual and exotic ways seem to be necessary for realizing Ag^{2+}. Balaya and Sunandana[31] looked at the EPR of Ag^{2+} formed during melt quenching of $60AgI-30Ag_2O-10B_2O_3$ glasses and correlated its temperature dependence to mobile ion dynamics and glass structure.

The observed, broadened EPR spectra (wiping out A anisotropy, etc.) possibly arise from the concentrated paramagnetic centers, namely, Ag^{2+} rather strongly coupled to the "matrix". The dipolar interactions are much larger than Zeeman and hyperfine terms. Dipolar interactions could broaden lines because of the local or internal magnetic field at a dipole produced by neighboring dipoles. As the transition between the different energy levels occurs, the arrangement of dipoles will change. Therefore, the internal magnetic field will vary from dipole to dipole also with time at a given dipole. For a dipole of 1 μ_B, this field is $\sim$1000 G.[32] These broadened lines completely mask individual g and A "principal" features in the observed EPR spectrum. Thus, the g and A features are not resolved. The standard parameters average g value (g), line width (ΔH_{PP}), and intensity (I_{PP}) which are extracted from temperature-dependent EPR spectra are plotted as a function of temperature for broad, asymmetric signal "A" shown in Figure 4c.

When pure AgI is heated, a strong, linear increase in intensity is observed until below the phase transition temperature. The intensity and line width suddenly drop at 423 K signaling the fact that a large fraction of paramagnetic complexes become diamagnetic as a result of the collapse of the cation sublattice and the associated local changes in the Ag−I bonding create a field of force that causes ion movement from the nonsuperionic to superionic phase and its effect on the magnetic susceptibility of AgI. When the sample is cooled, the EPR intensity is retraced confirming the reversibility of the structural phase transition. A smooth increase in the intensity (I_{PP}) perceived below phase transition temperature signifies that the affinity of silver and iodine increases with increasing temperature, which would tend to produce a decrease in volume. As a matter of fact, silver iodide contracts when heated and thermal hysteresis is (422.7−414.6 K = 8.1 ($\pm$1) K) in fact observed while cooling through the phase transition temperature. The average g value decreases smoothly from 2.2102 to 2.1133 and then suddenly drops to 2.0256 at 423 K which implies that the electrons become freer at T_t. Because α-AgI is a strongly anharmonic crystal, anhar-

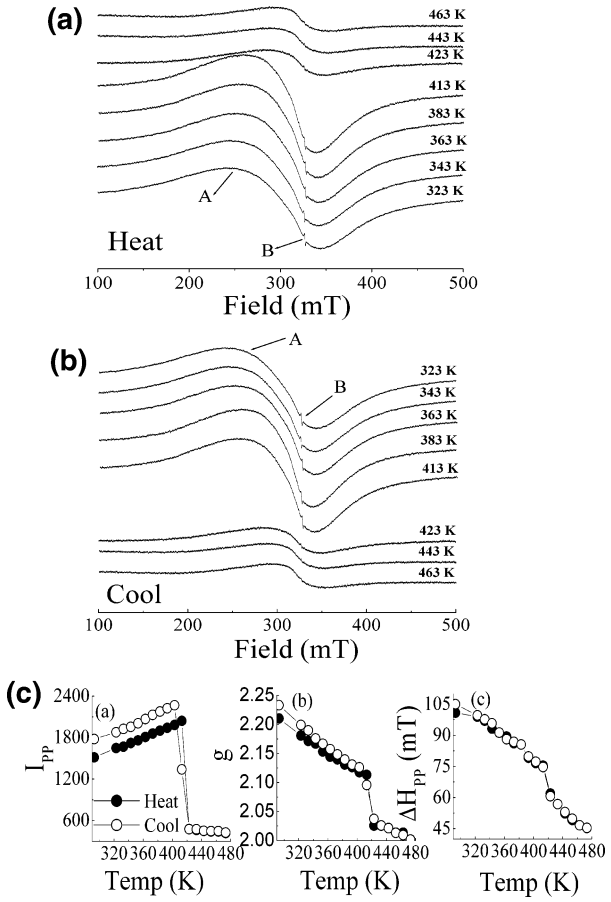

Figure 4. (a) Temperature dependence of EPR spectra of AgI nanocrystallites as they are warmed through the $\gamma \rightarrow \alpha$ phase transition. Note a drastic reduction in the intensity of signal "A" and disappearance of signal "B" in the α phase. (b) EPR spectra of AgI nanocrystallites as they are cooled from α phase to room temperature. Note the reversibility in phase transition and reproducibility of the spectra. (c) Abrupt changes in the intensity (I_{PP}), line width (ΔH_{PP}), and g values are observed at the phase transition temperature ($T_t = 423$ K) for the Ag^{2+} (signal "A") center on both heating and cooling cycles.

monic effects in the thermal vibration of atoms should be taken into account when analyzing ESR data. Note that line width decreases upon an increase of temperature. Therefore, the likely origin of line width is dipolar broadening rather than exchange broadening and can be attributed to cation motions which have a strong correlation with the chemical shifts.

As a result of MCR, a considerable number of Ag^+ interstitials and vacancies are produced by the intersection of dislocations, decomposition of dislocation dipoles, and nonconservative motion of dislocations[33] cited in ref 34. But among these two possible defects, Ag^{2+} interstitial needs much less energy and a closer iodine neighborhood when compared to vacancies for the paramagnetic defects formation. A fraction of the total number of Ag^+ interstitials in "off-center" positions stabilizes itself by sharing its d-electron and becomes a hole center. The rest of them could be responsible for the Ag^0-based paramagnetic centers and genuine interstitials (discussed later). CW microwave power saturation experiments have been performed at room temperature for signals "A" and "B" by varying microwave power from 5 to 170 mW. Plots of $I_{pp}(\Delta H_{pp})^2$ vs the square root of power (Figure 5) show an initial linear rise in signal "A", which would possibly arise from such an Ag^{2+}-based paramagnetic hole center. These hole centers are produced in the bulk level. A careful comparison made with the work of Senna et al. suggests that such behavior is observed

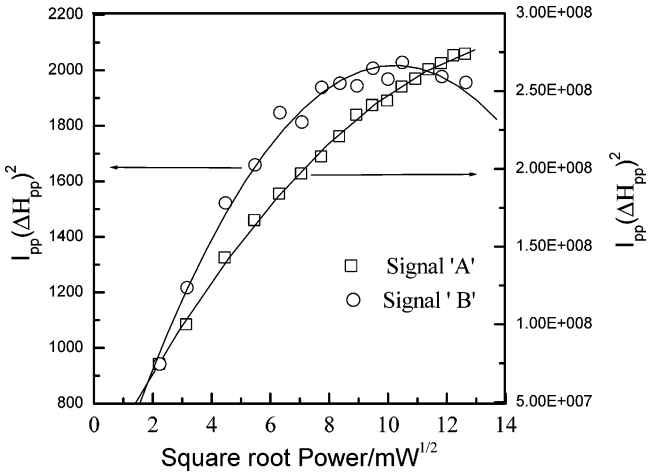

Figure 5. $I_{pp}(\Delta H_{pp})^2$ vs square root of microwave power for signal "A" and signal "B" as mentioned in parts a and b of Figure 4 shows the power saturation behavior of an Ag^{2+}-based hole center and Ag^0-based electron center, respectively.

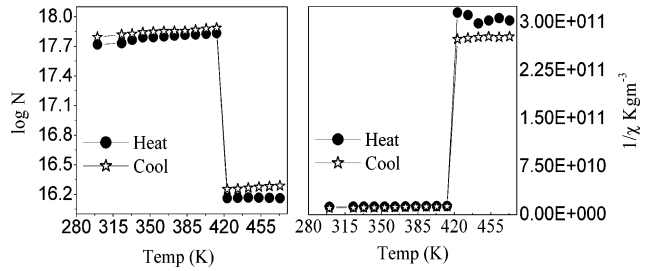

Figure 6. (a and b) Temperature dependence of the number of paramagnetic centers (N) and reciprocal susceptibility ($1/\chi$) corresponding to signal A in MCR-synthesized AgI. Note the abrupt changes at the phase transition temperature.

only for bulk centers/defects[35] indicating that signal "A" represents a hole center stabilized in the bulk.

Generally, the diamagnetic susceptibility χ of a semiconducting material is larger in the disordered than in the crystalline state. This variation of χ reflects changes in the local bonding configuration of the material depending upon the short-range order. In the superionic conductors, the bonding configuration changes (gradually for $T < T_t$ and suddenly at T_t) from pseudoionic to ionic with temperature due to defect formation and increasing thermal motion as reflected in the large Debye−Waller factor and ion disorder. Measurements of the number of spins (N) and paramagnetic susceptibility (χ) on the MCR-derived AgI from room temperature to above phase transition temperature are shown in Figure 6.

The number of spins participating in the resonance is calculated with the help of a reference (standard) $CuSO_4 \cdot 5H_2O$ by using the following formula from Weil et al.[36]

$$N_x = \frac{A_x(\text{scan}_x)^2 G_{\text{std}}(B_m)_{\text{std}}(g_{\text{std}})^2[S(S+1)]_{\text{std}}(P_{\text{std}})^{1/2}}{A_{\text{std}}(\text{scan}_{\text{std}})^2 G_x(B_m)_x(g_x)^2[S(S+1)]_x(P_x)^{1/2}} N_{\text{std}} \quad (1)$$

where A_x is the area under the absorption curve which can be obtained by double integrating the first derivative curve of signal A for different temperatures after a least-squares fit to an asymmetric Lorentzian function. "Scan" is the magnetic field corresponding to the unit length of the chart, G is the gain, B_m is the modulation field width, g is the splitting factor, S is the spin of the system in its ground state, and P is the microwave power. The subscripts "x" and "std" represent the corresponding quantities for the unknown sample (AgI) and reference,

respectively. Figure 6a shows a plot of log N against $1/T$ for the nanocrystalline AgI. It shows that there is a sudden drop in the number of spins of Ag^{2+} at the superionic phase transition from γ-AgI to α-AgI. The paramagnetic susceptibilities can be calculated from the EPR data by using the formula

$$\chi = \frac{Ng^2\beta^2 J(J+1)}{3k_B T} \quad (2)$$

where N is the number of spins per cubic meter and the rest of the symbols have their usual meaning. N can be calculated using eq 1, and g is taken from the EPR data. By the use of the above equation, paramagnetic susceptibilities were calculated at various temperatures. A plot of reciprocal susceptibility ($1/\chi$) as a function of absolute temperature (T) is shown in Figure 6b. Note the sudden jump in $1/\chi$ at the phase transition temperature which reflects the changes in the local bonding configuration of the material with temperature due to defect formation and thermal motion of Ag^{2+} ions which converts into an Ag^+ ion by trapping an electron from the neighbor Ag^0 to become a diamagnetic phase.

Electron Excess Center (Ag^0). A weak, narrow isotropic peak with the line width $\Delta H_{PP} = 12$ G (± 0.1 G) develops at $\langle g \rangle = 2.0019$ (± 0.0001) which is very close to the free electron value. This signal appears only after prolonged grinding (after 7 h) which corroborates with the XRD evidence for a minor phase and is also in accordance with the TEM observation. Since signal B at $\langle g \rangle = 2.0019$ is very close to the free electron value, it could arise from the conduction electron paramagnetic resonance (CEPR) due to the presence of Ag metal (Ag^0) nanoclusters on the surface or interface of the nanocrystalline γ-AgI produced by MCR. The CESR spectra of small metal particles are expected to exhibit very different behavior from those of bulk metals and are expected to depend on particle size. Two related effects such as surface and quantum effects modify the properties of small particles in comparison with bulk properties because of the validity of the discrete energy-level picture in small clusters. The ratio of the number of atoms at the surface of a small cluster to the number of inner atoms is of the order of $4(N)^{-1/3}$, where N is the total number of atoms in the clusters. Thus, for a 10 000-atom particle, the ratio is 6, an indication of surface effects arising for even moderately small particles. The major size dependence of the CESR g shift comes from a surface effect.[41] This could be compared to the work of Chen et al. who detected an ESR signal from electron centers in zeolite-Y after UV irradiation on an AgI/Y system at $g = 2.0020$ which is very close to the F center (2.0036).[37] The possible mechanism for the formation of Ag nanoclusters could be the partial collapse of mobile Ag^+ interstitials with electron capture from nearby I, which occurs upon grinding because MCR is very heterogeneous due to the stochastic nature involving a smooth convex surface and rather soft ingredients (Ag and I) producing a sliding type of motion under the influence of shear forces. This sliding causes the excitation of atomic motion at the interfaces, bulk deformation along slip planes leading to the excitation of atomic motions, and formation of defects. These centers are formed at the surfaces/interfaces and sensitive to microwave power. It is true that impurities could result from contamination of MCR equipment. However, our experiment involved a smooth-surfaced (essentially nonabrasive) agate mortar and pestle, using which we ground manually rather soft Ag (Moh's hardness 2.5−2.7) and flaky iodine. The hand-based grinding was rather slow—about 20−25 revolutions per minute. In view of these rather mild conditions, one could safely exclude equipment-based impurities getting into the MCR samples. Under these circumstances, the contamination due to agate mortar may not lead to EPR signals that are very sharp and strong in comparison with signal "B". Such impurities—even if present—are apparently below the detection limit of our EPR spectrometer. In this context, we would confirm that signal 'B' possibly arises from the Ag^0 paramagnetic center.

In view of the discussion from the previous section, another fraction of Ag^+ interstitials becomes Ag^0 paramagnetic centers after a capture of electrons from near by iodines and further move to the surface by the action of continuous deformation/dislocations during the MCR. The Ag^0 center reflects as signal "B" in parts a and b of Figure 4. To fully assign this signal "B", a microwave power saturation method was employed. The power saturation behavior of signal "B" indicates that this signal begins to saturate at ~16 mW and the saturation is complete at ~80 mW, to be clearly distinguished from the still-rising signal "A" at the latter power. A careful qualitative comparison of this feature with those of Senna et al. suggests that signal B is possibly due to the presence of Ag^0-based paramagnetic centers, perhaps related with surface defects.[35] The relatively large power needed for the saturation of signal B may have its origin in the skin depth of the Ag^0 clusters. The resonance line of Ag^0 is almost isotropic and moreover it has a relatively small intensity, since the unpaired electrons involved exist near the Fermi level. This line intensity is almost independent of temperature. Because of the good conductivity property of a metal, the penetration of the microwave radiation is limited. However, there is a small shift in the g value (from 2.0019 to 2.0054) and ΔH_{PP} (from 10 to 7 G) with increasing temperature believed to be the result of spin−orbit interaction coupling which can be correlated with the cluster size. Elliott[38] and Yafet[39] emphasized the importance of the spin−orbit potential in the spin relaxation process. Elliott has established a relation, $T_2 \sim \tau/\Delta g^2$ where T_2 is the spin relaxation, τ is the scattering rate, and Δg is the g shift for the spin−orbit independent scattering potentials. It was predicted that the Elliott relaxation mechanism would be quenched in a small enough particle and that the CESR lines would thus be narrow and have long relaxation times. This problem was addressed by Kawabata,[40] who studied the size dependence of the g shift in small metallic particles, the g shift contains a contribution which adds to the bulk g shift and which is proportional to L^2, where L is the average particle diameter. Later, Buttet et al.[41] developed an orthogonalized standing wave formalism which reexamined the behavior of the g shift as a function of particle size, and they compared the predictions of this formalism with existing experimental data: the difference (g shift, Δg) between the g value of the metal considered and the free electron g value (2.0036) is a rough measure of the spin−orbit potential magnitude. In this present work, the g shift ($\Delta g = -4 \times 10^{-4}$) is calculated for 10 nm sized Ag metallic clusters which lies between those of atomic (-8×10^{-5}) and bulk ($(-1.9 \pm 0.1) \times 10^{-2}$) values.[41] In these metals, the g shift should thus increase in magnitude from its atomic value to its bulk value as the particle size increases. The Buttet model predicts g shift changes from the bulk value of 20% and 8% for 20 A^0 and 50 A^0 particles, respectively. On the other hand, Kawabata's theory predicts changes of 1% and 9% for the same particles. Unfortunately, all of these predicted changes are within the experimental error of the measurements. More generally, all aspects of conduction electron paramagnetic resonance in small clusters, including relaxation times and line widths, need further experimental study so that the behavior of such particles in quantum size effect regime can be better understood. This

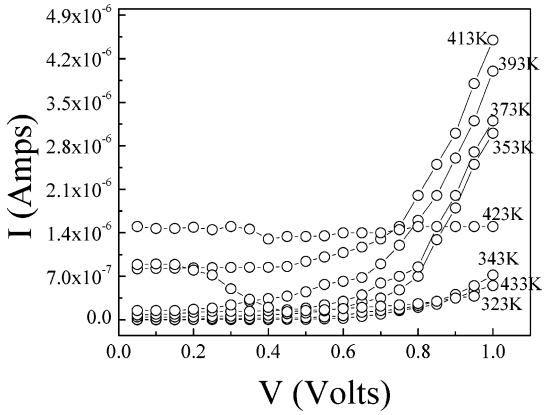

Figure 7. *I*−*V* characteristics of MCR-derived AgI shows nonlinear behavior until below the T_t (423 K). Current increasing nonlinearly with increasing temperature indicates the creation of electronic defects such as Ag^0-type clusters.

signal "B" appears even after the phase transition temperature with much less intensity. The reasons could be the migration of metallic particles to the Ag−I crystallite surface where bigger metallic particles are formed. This happens only when there is a change in the chemical bonding by means of changes in the coordination number of Ag atoms, symmetry, geometrical structure, and configuration of the d-orbital in the α-AgI structure. The α-AgI structure is the one in which nearly complete Frenkel disorder in the silver sublattice occurs between 150 and 555 °C with a very small fraction of Schottky defects. Temperature dependence of EPR observed in the present case strongly favors an Ag-to-I composition ratio slightly in excess of unity in the form of (Ag−I) charged clusters as part of a regular nanostructure. Otherwise, Ag-based EPR would not reflect a structural phase transition on a microscopic scale as observed in the present work. Furthermore, the production of paramagnetic clusters by MCR and EPR of probing the AgI phase transition is a "nonlocal" kind of EPR which acts as a local probe of the interactions of spin magnetic moment of the impurities with its immediate neighbors. It is to be noted that both the conducting Ag^+ and the paramagnetic Ag^{2+} belong to one and the same sublattice. It is reasonable to suppose that the randomly distributed Ag^{2+} impurity complexes sense the dynamics of the Ag^+ sublattice. Fluctuations in this sublattice are essentially electromagnetic. It is the fluctuations which are root of the phase transition. These electromagnetic interactions are intricately coupled to Ag^+ ion dynamics allowing EPR to sense the dynamic distortions associated with the cation sublattice. Further information about such distortions must await detailed theoretical and computational studies of cluster geometry and dynamics.

Interestingly, EPR results bear an important comparison to the dc electronic conductivity measurement carried out with the aid of a constructed dc two-probe Hebb−Wagner[42,43] polarization cell.[4] A nonlinear current or nonohmic behavior is observed until below the T_t (423 K) (Figure 7). But a linear (ohmic) behavior is seen at 423 K with the current on the order of 10^{-6} amps due to the partial phase transformation of $\gamma \rightarrow$ α-AgI, and thereafter the linear current decreased to 10^{-9} A. In other words, it transforms from an electronic solid to ionic solid at above T_t. An increased nonlinear current with increasing temperature indicates the creation of electronic defects. These are formed at the interfaces and probably act as microscopic p−n junctions as a direct result of the MCR as reflected in the form of signal B. This study therefore underlines the importance of electronic defects for the formation and stability of nanoparticles especially in a unique process such as mechanochemical synthesis.

Finally, we will say that the new structures are probably generated during the MCR process because of the creation of a substantial concentration of generic defects such as Ag^+ vacancies and interstitials. These defects are mobile and Ag^+ interstitials are valuable to electron capture. The MCR process takes at least 5−10 h to complete. During this period, the following could take place: (a) interfacial diffusion of ion and/electron occuring at solid−solid and solid−vapor interfaces, (b) the deformation or breaking up of Ag depending on whether it is (111), (200), or (311), and so forth, into unstable fragments, (c) the formation of AgI_4 and IAg_4 clusters among others, in general, one could think of (Ag_x-I_y) clusters, (d) the ordering of these clusters and birth and stabilization of Frenkel defects, and (e) the formation of AgI phases. Given the leisurely nature of the formation process and the propensity of Ag−I for unusual cluster formation, it would be reasonable to expect that, as a way to form Frenkel defects, locally stable paramagnetic defects with a net 2+ charge are realized in sufficient number to give a broad, asymmetric EPR spectrum (signal "A"). In addition, one may also have unreacted Ag in the form of nanocrystallites or semimetals as discussed earlier indicating a sharp signal "B" in the EPR spectrum. Gurin[44] has performed ab initio calculations of energy levels of Ag_xI_y clusters. It appears that the geometry of these clusters can easily be altered due to the appearance of dangling bonds and atoms with coordinates less than 4. MCR can probably create dangling bonds in AgI during the process because of the relatively high ionicity, polarizability, and the contribution of d-orbital electrons too. These properties can alter such clusters rather easily to create paramagnetic defects such as those detected by present EPR studies.

Conclusions

X-band EPR spectra of nanocrystalline (∼40 nm) AgI synthesized by MCR and characterized by XRD and TEM yield two process-related, Ag-based EPR signals: a broad asymmetric hole center with $\langle g \rangle = 2.21025$ and $\Delta H_{PP} = 1000$ G and a sharp electron center with $\langle g \rangle = 2.0019$ and $\Delta H_{PP} = 10$ G. The two signals successfully probe the superionic phase transition (on a microscopic scale) from low-temperature zinc blende (γ) phase to a high-temperature superionic conducting (α) phase at 423 K. $\langle g \rangle$, ΔH_{PP}, and integrated intensity all show abrupt drops at the transition temperature. Phase transition thermodynamics as probed by DSC support the ESR results. The phase transition is characterized by a sharp abrupt rise in the inverse paramagnetic susceptibility $1/\chi$ at the transition temperature. Thus, the present EPR study together with high-temperature electronic conductivity behavior shows that the creation of electronic defects is necessary for the formation of γ-AgI nanoparticles in a near-equilibrium process such as the MCR.

Acknowledgment. We thank Dr. R. Ramani, Helsinki University of Technology, Espoo, Finland, and Mr. D. D. Gore, Armed Forces Medical College, Pune, for electron microscopic characterization. Sincere thanks are due to the University of Hyderabad for the award of a research fellowship to D. Bharathi Mohan under the UPE program.

References and Notes

(1) Chandra, S. *Superionic Solids: Principles and Applications*; North-Holland: Amsterdam, The Netherlands, 1981.

(2) Aniya, M.; Ichihara, S. *J. Phys. Chem. Solids* **2005**, *66*, 288.

(3) Sunandana, C. S.; Senthil Kumar, P. *Bull. Mater. Sci.* **2004**, *27*, 1.

(4) Bharathi Mohan, D.; Sunandana, C. S. *J. Phys. Chem. Solids* **2004**, *65*, 1669.
(5) Heinicke, G. *Tribochemistry*; Akademie-Verlag: Berlin, Germany, 1984.
(6) Jost, H.; Hennig, H. P.; Ebert, I.; Jedamzik, J. *Proceedings of the 10th International Symposium on Reactivity of Solids*; Dijon, France, 1984.
(7) Badalyan, A. G.; Zhitnikov, R. V. *Sov. Phys. Solid State* **1985**, *27*, 1774.
(8) Walters, G. K.; Estle, T. L. *J. Appl. Phys.* **1984**, *32*, 1854.
(9) Golubev, V. V.; Evdokimov, V. B. *J. Phys. Chem.* **1964**, *38*, 477.
(10) Hoffman, K.; Hahn, D. *Phys. Status Solidi A* **1974**, *24*, 637.
(11) Kakazey, M.; Vlasova, M.; Ristich, M.; Srechkovich, T. *Proceedings of the First APES Symposium*; Rudowicz, C. Z., Ed.; Hong Kong, 1997.
(12) Assabghy, F.; Arafa, S.; Boulos, E.; Bishay, A.; Kreidl, N. J. *J. Non-Cryst. Solids* **1977**, *23*, 81.
(13) Nistor, S. V.; et al. *Phys. Status Solidi B* **1994**, *185*, 9.
(14) Bastow, T. J.; Whitfield, H. J.; Cockman, R. W. *Solid State Commun.* **1981**, *39*, 325.
(15) Smith, M. J. A.; Ingram, D. J. E. *Proc. Phys. Soc., London* **1962**, *80*, 310.
(16) Janssen, G.; Bowen, A.; Goovaerts, E. *Phys. Rev. B* **2005**, *71*, 035415.
(17) Spoonhower, J. P.; Marchetti, A. P. *J. Phys. Chem. Solids* **1990**, *51*, 93.
(18) Richards, P. M. *Physics of Superionic Conductors*; Salamon, M. B., Ed.; Springer-Verlag: 1979; Chapter 6, p 141.
(19) Cullity, B. D. *Elements of X-ray Diffraction*; Addision-Wesley: Philippines, 1978.
(20) Wang, Y.; Wang, W.; Fan, K.; Deng, J. *Surf. Sci.* **2001**, *48*, *7* 77.
(21) Kvist, A.; Josefson, A. M. *Z. Naturforsch.* **1968**, *23*, 625.
(22) Ishii, T.; Kamishima, O. *J. Phys. Soc. Jpn.* **1999**, *68*, 3580.
(23) Nolting, J.; Rein, D. *Z. Phys. Chem. Neue Folge* **1969**, *66*, 150.
(24) Senthil Kumar, P.; Kini, N. S.; Umarji, A. M.; Sunandana, C. S. *J Mater. Sci.* 2005, in press.
(25) Takahashi, H. *J. Phys. Soc. Jpn.* **1987**, *56*, 2520.
(26) Shaviv, R.; Westrum, E. F.; Gronvold, F.; Stolen, S.; Inaba, A.; Fuji, H.; Chihara, H. *J. Chem. Thermodyn.* **1989**, *21*, 631.
(27) Kundu, T. K.; Manoharan, P. T. *Mol. Phys.* **2000**, *98*, 2007.
(28) Senthil Kumar, P.; Sunandana, C. S. *Thin Solid Films* **1998**, *323*, 110. Senthil Kumar, P.; Babu Dayal, P.; Sunandana, C. S. *Thin Solid Films* **1999**, *357*, 111.
(29) Senthil Kumar, P.; Balaya, P.; Goyal, P.; Sunandana, C. S. *J. Phys. Chem. Solids* **2003**, *64*, 961.
(30) Fischer, P.; et al. *J. Phys. Chem. Solids* **1971**, *32*, 1641.
(31) Balaya, P.; Sunandana, C. S. *Solid State Ionics* **1990**, *40*, 700.
(32) Van Vleck, J. A. *J. Chem. Phys.* **1937**, *5*, 320.
(33) Batsanov, S. S. *Usp. Khim.* **1968**, *37*, 778.
(34) Vainshtein, B. K.; Fridkin, V. M.; Indenbom, V. *Modern Crystallography II: Structure of Crystals*; Springer-Verlag: Berlin, Germany, 1982; Vol. 21, p 348.
(35) Watanabe, T.; Isobe, T.; Senna, M. *J. Solid State Chem.* **1996**, *122*, 291.
(36) Weil, J. A.; Bolton, J. R.; Wertz, J. E. *Electron Paramagnetic Resonance: Elementary Theory and Practical Applications*; Wiley: New York, 1994; p 498.
(37) Chen, W.; Joly, A. G.; Roark, J. *Phys. Rev. B* **2002**, *65*, 245404.
(38) Elliott, R. J. *Phys. Rev.* **1954**, *96*, 266.
(39) Yafet, Y. *Solid State Phys.* **1963**, *14*, 1.
(40) Kawabata, A. *J. Phys. Soc. Jpn.* **1970**, *29*, 902.
(41) Buttet, J.; Car, R.; Myles, C. W. *Phys. Rev. B.* **1982**, *26*, 2414.
(42) Hebb, M. M. *Chem. Phys.* **1952**, *20*, 185.
(43) Wagner, C. *J. Electrochem. Soc.* **1956**, *60*, 4.
(44) Gurin, V. S. *Int. J. Quantum Chemistry* **1999**, *71*, 337.